A Theoretical Study of Bonding in Lanthanide Trihalides by Density Functional Methods

Carlo Adamo† and Pascale Maldivi*

Département de Recherche Fondamentale sur la Matière Condensée, Service de Chimie Inorganique et Biologique, Laboratoire de Reconnaissance Ionique, CEA-Grenoble, 17 Rue des Martyrs 38054 Grenoble Cedex 9, France

Received: January 22, 1998; In Final Form: May 20, 1998

Theoretical investigations of LnX_3 systems (Ln = La, Gd, Lu and X = F, Cl, Br, I) have been carried out by various density functional methods, including nonlocal gradient corrections and self-consistent hybrid density functional/Hartree−Fock approaches. The relativistic effects were taken into account either by a relativistic effective core potential (RECP) or within a frozen core approximation and a quasi-relativistic approach for the valence electrons, either scalar or including the spin−orbit contribution. Geometry optimizations and harmonic frequencies calculations were carried out, as well as computation of the atomization energies. All data were found to be in very good agreement with experimental data, being at least of the same quality as other RECP-based post-Hartree−Fock calculations. The conformation was found to be pyramidal for the lighter lanthanides and halogens and planar for $GdBr_3$, GdI_3, $LuCl_3$, $LuBr_3$, and LuI_3. Special attention was also devoted to the description of the lanthanide−halogen bond, depending on the hardness of these atoms. The bonding was examined in terms of contributions of the lanthanide atomic orbitals to the molecular orbitals of the LnX_3 species. Charges were calculated through the natural population analysis procedure, and some investigations have been carried out using the natural resonance theory, as implemented in the framework of the natural bond orbital approach. An energetic analysis based on the transition state method of Ziegler et al. was also performed and gave the energetic contributions (i.e., steric, electrostatic, and orbital) to the bonding. All these analyses point to a highly ionic interaction, especially for the lighter halogens and lanthanides, even if some non-negligible ligand-to-metal charge transfer occurs with the more polarizable bromine and iodine. Nevertheless, the stabilization brought by this covalent charactacter is weak compared to the stabilization due to electrostatic interactions.

1. Introduction

Electronic structure of molecular systems containing f elements has been the object of numerous experimental[1−3] and theoretical studies.[4−8] In this framework, one of the more challenging topics is the "chemical" description of the lanthanide−ligand or actinide−ligand interactions in terms of ionic vs covalent interaction.[8,9] This point is of great importance for a better understanding of the molecular properties of lanthanide and actinide series, such as stability or reactivity. For instance, the improvement of chemical processes involved in the nuclear waste treatment may be expected from a better basic description of these interactions.[10] Theoretical investigations are therefore useful to get more insight into the lanthanide or actinide−ligand interactions within various kinds of molecular environments.

Unfortunately, a precise evaluation of molecular properties is still far from being a routine task, especially when f electrons are involved. In fact, a reliable theoretical tool must be able to yield, at the same time, precise geometrical and thermodynamic results and a detailed "chemical" analysis of the electronic structure. Such a tool requires a sufficiently accurate treatment of the two main physical effects that dominate the chemistry and physics of heavy metals, i.e., relativity and electron correlation.

Different relativistic contributions play a significant role in heavy metal chemistry[11] and can be described by different approaches (see ref 12 for a comprehensive recent review), ranging from four component fully relativistic Dirac−Fock methods,[13−15] to two-component approximations resulting from the Foldy−Wouthuysen (FW)[16] or the Douglas−Kroll[17] transformations of the Dirac Hamiltonian, to the very cheap and popular relativistic effective core potential (RECP) approaches.[18−21]

The development of accurate functionals, including gradient corrections, makes the approaches rooted in the density functional theory (DFT) the most powerful nonempirical alternative to conventional Hartree−Fock (HF) and post-HF methods.[22] A number of studies[23−26] show that DFT methods based on the generalized gradient approximations (GGA) can model with remarkable accuracy the properties of heavy transition metals. Even better results can be obtained by the so-called self-consistent hybrid (SCH) approaches.[27−30] Furthermore, these methods are particularly powerful for a chemist, since their monodeterminantal nature allows an easy-to-read interpretation of the results. As a consequence, standard "chemical" analysis tools, originally developed for the HF scheme, can be applied.[28]

The implementation of relativistic models in the DFT framework has been achieved at different precision levels, such as the perturbational treatment of a FW operator[31] or the zero-order regular approximation (ZORA).[32] Furthermore, it has been shown that standard RECP's provide accurate description also in DFT schemes.[33]

* Corresponding author. E-mail: pmaldivi@cea.fr.
† Permanent adress: Dipartimento di Chimica, Università della Basilicata, Via N. Sauro 85, I-85100 Potenza, Italy. E-mail: adamo@pzuniv.unibas.it.

S1089-5639(98)00840-8 CCC: $15.00
Published on Web 07/31/1998

The above-mentioned studies document that DFT methods are able to capture the main features of metal−ligand interactions, at least for complexes involving first- and second-row transition metals. The situation is more crucial for Ln and An complexes, since the reliability of DFT methods in describing on the same footing correlation and relativistic effects[12] has not been fully proved. In fact, only few investigations have yet been carried out on small model systems, such as lanthanide oxides.[34]

We thought it interesting to investigate whether SCH and GGA approaches provide a sufficiently reliable description of the bonding in Ln(III) compounds. In particular, two different approximations were chosen to take into account relativistic effects: either the RECP model[21] or a frozen core description combined with the quasi-relativistic treatment of the valence electrons.[35−38]

The LnX_3 model compounds (X = F, Cl, Br, I) were found to be good candidates for our purpose, as they have been the subject of numerous experimental studies[2,3,39−43] and several recent theoretical investigations have appeared in the literature.[41,43−48] Moreover, the use of halogen ligands leads to a modulation of the chemical environment of the lanthanide from a hard anion (F^-), to a soft, polarizable ion (I^-), providing a useful framework for further analysis of the electronic structure in terms of ionic vs covalent bonding. We have investigated three lanthanides, namely, La, Gd, and Lu, chosen among the whole series because the electronic configuration of their trivalent state is $4f^0$, $4f^7$, and $4f^{14}$, respectively; thus, they do not exhibit any first-order spin−orbit (SO) coupling. In the case of Gd(III), no second-order SO coupling may be expected, as the first excited state is very high above the ground state.

2. Computational Details

Two different implementations of the Kohn−Sham (KS) approach have been used. In the first one, a quasi-relativistic methodology has been chosen, as developed in the Amsterdam density functional package (ADF 2.3.0),[37,49] where the atomic core electronic density is obtained via a fully relativistic Dirac Slater (DS) calculation. The valence eigenfunctions and eigenvalues are obtained by a quasi-first-order perturbative treatment of the main relativistic (mass−velocity and Darwin) terms developed upon nonrelativistic Slater type orbitals.[31] Calculations were also performed with the *jj* coupling scheme, i.e., making use of the double group symmetries.

The exchange and correlation potentials were included either in the local spin density approximation (LSDA) using the exchange energy of the uniform-electron gas[50] with the parametrization of Vosko, Wilk, and Nusair[51] for the correlation counterpart or within the GGA scheme. In this latter case, a number of different correlation functionals were considered, namely, the functional developed by Lee,Yang, and Parr (LYP),[52] by Perdew[53] (P), or by Perdew and Wang (PW).[54] These functionals were used, in a self-consistent procedure, with either the Becke[55] (B) or Perdew-Wang (PW)[54] exchange functional. Following the standard acronyms, the methods will be referred in the following as LSDA, BLYP, BP, BPW, and PW (abbreviation for PWPW), respectively.

The evaluation of the various energetic contributions to the total binding, i.e., Pauli repulsion, electrostatic, and orbital interactions, was carried out through the generalized transition-state method of Ziegler[56] et al. In this approach the different contributions are estimated with respect to starting fragments, and we have chosen the ionic species, Ln^{3+} and X^-, as these reference fragments.

The valence space of all the atoms, including the 5s, 5p, 4f, 6s, and 5d electrons for lanthanides and the $ns^2\ np^5$ electrons of halogens, was described by Slater type orbital (STO) basis set of triple quality. One single d polarization function was also added for halogens.[57] Auxiliary sets of STO functions were used for all the atoms to fit the molecular density and to generate the Coulomb and exchange potentials.[58]

The second DFT approach is based on a SCH method, obtained by a combination of HF and Becke[55] exchange with the Perdew[53] correlation functional. The ratios of the different contributions are those optimized by Becke for a closely related, althought not identical, functional.[30] We will refer to this SCH method as B3P. The RECP's of Cundari and Stevens[21,59] have been used for both the lanthanide and the halogen atoms. These RECP's explicitly treat the 5s, 5p, 4f, 6s, and 5d electrons of the lanthanides by a contracted basis set of Gaussian type orbitals (GTO) with a (3111/3111/21/52) pattern for Gd and Lu and a (52111/5211/311) pattern for La. A single f polarization function (0.261) was also added for La. The valence space of the halogens includes the *n*s and *n*p electrons, and it is described by a polarized double basis set.[59,60] All SCH computations have been carried out using the Gaussian 94 program.[61]

All the geometries have been fully optimized both in pyramidal (C_{3v}) and planar (D_{3h}) conformations using an energy-only minimizer, and the resulting geometries characterized by computing second derivatives by a double numerical derivation.

Finally, the electronic structures of these model systems, obtained by SCH computations, have been investigated using the natural population analysis (NPA).[62] Further analysis on the LnX_3 electronic structure has been carried out throughout the natural resonance theory (NRT),[63] which provides a molecular electron density analysis in terms of classical resonance theory concepts.

3. Results and Discussion

Atomic Calculations. Before performing molecular calculations, we have checked the DFT approaches on a set of atomic data of La, Gd, and Lu, i.e., atomic orbital eigenvalues and ionization potentials (IP). In this connection, it is now well-established that the KS orbitals are a well-defined approximation to the HF orbitals.[64,65] From a chemical point of view, a number of studies has shown that overall trends (e.g., IP, orbital eigenvalues, electron affinities) are well-reproduced (see for instance refs 31 and 66) compared to those obtained from HF methodology.

Table 1 collects the orbital energies of the considered Ln atoms, evaluated by the scalar relativistic Hamiltonian (Sc) or by including the SO (*jj*) coupling. As it appears from these data, all the approaches are able to reproduce the main trends regarding the evolution of the 5d, 6s, and 4f orbitals when going from La to Lu. These evolutions, generally explained by shell structure and relativistic effects,[67] are due to the increase of the nuclear effective charge when filling the 4f orbitals, which stabilizes the 6s orbital and destabilizes the outer 5d orbitals. The 4f orbitals also experience the increased effective nuclear charge, getting more core like orbitals when going to the end of the lanthanide series. Our LDA/SO calculations satisfactorily reproduce the four-component relativistic LDA (RLDA) results.[66] Similarly, the GGA/SO computations give a good agreement with DS calculations. In this connection, methods including the P or the PW correlation functionals seem to perform better than that using the LYP functional.

TABLE 1: Orbital Eigenvalues (Absolute Values, eV) of the Ln Atoms, Computed Using Different DFT Approaches[a]

Ln	nonrel (BP)	LSDA Sc	BLYP Sc	BP Sc	PW Sc	BPW Sc	LDA SO	BLYP SO	BP SO	PW SO	BPW SO	DS	RLDA[b]
							La						
5p	22.62	22.33	23.14	22.37	22.31	22.29	23.59	24.47	23.61	23.56	23.54	23.46	24.23
							21.46	22.33	21.49	21.43	21.41	20.90	21.68
4f	7.5	4.07	4.99	3.96	3.90	3.87	4.11	5.07	3.40	3.94	3.91	4.06	
							3.87	4.83	3.76	3.70	3.67	3.78	
5d	4.07	3.35	3.93	3.38	3.30	3.28	3.24	3.92	3.23	3.15	3.13	2.55	3.34
							3.08	3.76	3.07	2.99	2.96	2.36	3.15
6s	3.73	3.97	4.38	3.99	3.30	3.88	3.83	4.36	3.83	3.73	3.71	3.14	3.80
							Gd						
5p	27.64	28.09	28.73	28.14	28.07	28.04	29.76	30.65	29.77	29.72	29.69	29.60	30.39
							25.86	26.73	25.86	25.81	25.78	25.19	26.02
4f	9.31	10.21	10.92	10.18	10.13	10.08	8.69	9.62	8.58	8.53	8.49	8.45	9.48
							7.99	8.91	7.88	7.83	7.79	7.68	8.72
5d	3.93	3.06	3.56	3.05	2.96	2.92	2.74	3.43	2.70	2.62	2.58	2.05	2.87
							2.50	3.18	2.46	2.38	2.34	1.79	2.60
6s	4.13	4.51	4.94	4.53	4.43	4.41	4.27	4.84	4.26	4.17	4.14	3.56	4.25
							Lu						
5p	30.50	31.67	32.49	31.67	31.64	31.59	35.63	36.52	35.63	35.60	35.55	35.91	36.63
							29.60	30.46	29.58	29.54	29.50	28.96	29.75
4f	15.32	9.50	10.39	9.38	9.35	9.30	10.27	11.17	10.16	10.12	10.07	9.96	10.81
							8.81	9.71	8.70	8.66	8.60	8.43	9.28
5d	3.02	2.03	2.57	2.02	1.94	1.90	1.97	2.64	1.92	1.85	1.79	1.32	2.14
							1.69	2.34	1.64	1.58	1.52	1.01	1.81
6s	4.41	5.00	5.46	5.03	4.94	4.92	4.79	5.39	4.79	4.70	4.67	4.06	4.78

[a] In the case of scalar spin density calculations, only the α-orbital energies have been reported. The atomic orbitals derived from SO calculations are listed with the l−1/2 term above the l+1/2 term. The following, lowest energy, electronic configurations have been taken: La, [Xe] $6s^2 5d^1$ or [Xe] $6s^2_{1/2}\ 5d^1_{3/2}$; Gd, [Xe] $6s^2\ 5d^1\ 4f^7$ or [Xe] $5d^1_{3/2}6s^2_{1/2}4f^6_{5/2}4f^1_{7/2}$; Lu, [Xe] $4f^{14}6s^25d^1$ or [Xe] $6s^2_{1/2}4f^6_{5/2}4f^8_{7/2}5d^1_{3/2}$. [b] From ref 66.

TABLE 2: Ionization Potential (eV) for the Considered Ln Atoms, Calculated with Scalar (Sc) or with Spin−Orbit (SO) DFT Approaches

		La	Gd	Lu
exptl[a]		5.58	6.15	5.42
LSDA	Sc	6.03	5.72	5.51
	SO[b]	6.31	6.85	5.59
	SO[c]	6.41	6.87	5.42
PW	Sc	5.73	6.04	5.34
	SO[b]	6.08	6.69	5.41
	SO[c]	6.18	6.72	5.24
BP	Sc	5.88	6.15	5.436
	SO[b]	6.25	6.82	5.49
	SO[c]	6.37	6.84	5.33
BLYP	Sc	6.92	7.34	6.21
	SO[b]	6.71	7.47	6.36
	So[c]	6.81	7.49	6.18
BPW	Sc	5.60	5.90	5.31
	SO[b]	6.02	6.66	5.38
B3P	Sc	6.78	7.03	4.39
DS[b]		5.63	6.12	4.87
DS[c]		5.77	6.12	4.68
RLDA[d]		6.26	6.83	5.52

[a] From ref 70. [b] From lowest energy *jj* subconfiguration [c] From averaged *jj* subconfigurations. [d] From ref 66.

The computed ionization potentials of La, Gd, and Lu are reported in Table 2, and they refer to the lowest energy electronic configuration (GGA and SCH results) or to the averaged subconfigurations (GGA results). In this last connection, it must be remembered that, for rare earth elements characterized by high spin and orbital quantum numbers, the determination of the states arising from the LS coupling becomes rather cumbersome. An approximate evaluation of the energy of a state with given LS has been proposed in the literature[68,69] by averaging the energies of all the *jj* subconfigurations generated from a LS state, weighing each energy by the degeneracy of the *jj* configuration. For example, the averaged energy of the ground state of La^+ (d^2, $^3F_2$) is

$$E_{av} = \frac{\sum_{jj\ \mathrm{conf}} (\sum 2J+1)\cdot E_{jj}}{\sum_{jj\ \mathrm{conf}} (\sum 2J+1)} = \frac{6E(d^2_{3/2}) + 15E(d^2_{5/2}) + 24E(d^1_{3/2}\ d^1_{3/2})}{45}$$

The Gd^+ ground state ($^{10}D_{5/2}$) leads to two possible *jj* subconfigurations: $4f^6_{5/2}\ 4f^1_{7/2}5d^1_{3/2}6s^1_{1/2}$ and $4f^6_{5/2}4f^1_{7/2}5d^1_{5/2}\ s^1_{1/2}$, whereas the Lu^+ configuration is $6s^2_{1/2}$ with no LS coupling. The energy of the ground states of the neutral atoms (d^1s^2 configuration) may also be averaged owing to the $d_{3/2}$ and $d_{5/2}$ splittings.

Our results show that the BLYP and B3P approaches give quite poor results, whereas the BP, PW and BPW protocols are more efficient to reproduce experimental data.[70] The inclusion of SO effects gives a worse agreement with experimental data for the earlier lanthanides La and Gd, whereas it is as good as, or better than, scalar calculations for the later element Lu. This trend is in order with the increase of relativistic effects, from the beginning to the end of the series. The differences are small anyway as the SO splitting of a d shell is small (≈0.14 eV[69]), compared to the SO effect experienced by a p shell for instance (≈1.1 for 5p shell in I[69]). Therefore *jj* coupling does not change much the overall quality of the computations in those particular cases.

Finally, and to further check the performances of DFT approaches, the $^2D_{3/2} - {}^2D_{5/2}$ splitting arising from the ground state of La has been calculated. As it is well-known, in this particular case, the resulting Slater determinant is also an eigenfunction of the LS operator. All the considered DFT protocols provide a good agreement with the experimental estimate (0.13 eV),[70] the values ranging between 0.16 eV (LDA, BP, and PW) and 0.17 eV (BLYP).

TABLE 3: Bond Lengths (*d*, Å) and Angles (Θ, deg) for the LnX_3 Series, Computed with GGA (BP/QR, BP/RECP) and SCH (B3P/RECP) Methods, Compared with Experimental[40,42] Data and Other Published RECP-Based Results: MC/SCF[41,46,47] and CISD+Q[44]

	BP/QR[a]		B3P/RECP		BP/RECP		CISD+Q	MC/SCF	exptl	
	d	Θ	*d*	Θ	*d*	Θ	*d*	*d*	*d*	Θ
LaF_3	2.124	114.8	2.177	115.4	2.168	112.7	2.159	2.176	2.22	120
$LaCl_3$	2.590	116.5	2.609	118.2	2.641	114.1	2.612	2.643	2.59 / 2.62	112.5/120
$LaBr_3$	2.740	116.3	2.754	118.1	2.779	114.6	2.770		2.74	115.5
LaI_3	2.983	119.4	2.969	117.8	2.993	114.4	3.016		*2.99*	
GdF_3	2.031	113.9	2.050	117.5	2.046	115.6	2.056	2.047	2.053	108.4
$GdCl_3$	2.481	119	2.519	120.0	2.515	120.0	2.511	2.528	2.489	113
$GdBr_3$	2.63	119.8	2.662	120.0	2.661	120.0	2.667	2.68	2.640	
GdI_3	2.868	120	2.887	120.0	2.893	120.0	2.903	2.91	2.84	
LuF3	1.968	117.8	1.985	118.5	2.003	117.3	1.965	1.985	*1.968*	
LuCl3	2.400	120	2.425	120.0	2.444	120.0	2.428	2.440	2.417	111.5
LuBr3	2.546	120	2.552	120.0	2.577	120.0	2.584	2.60	2.506	
LuI3	2.791	120	2.797	120.0	2.807	120.0	2.819	2.83	2.771	

[a] QR: quasi-relativistic treatment from ADF.

These results on atomic systems clearly point out the relevant role played by the correlation functional in determining the performance of DFT methods in heavy-metal systems. These effects can be related to a set of physical conditions that must be respected by a formally correct correlation functional.[71] In particular, three conditions play a determining role in chemical applications:

(a) the attainment of the exact limit of the uniform electron gas;

(b) the distinct treatment of parallel and antiparallel spin correlation;

(c) the attainment of exactly zero correlation energy in any one-electron system (e.g., H atom).

With respect to these requirements, the three chosen correlation functionals (LYP, P, and PW) have a different behavior. From one hand, the LYP functional has the correct behavior for one-electron systems but does not contain any correlation for electrons with parallel spins and does not have the right limiting behavior for uniform electron-gas systems. Despite these limitations, the LYP functional has been long considered as a reference point in DFT computation of organic systems.[72,73] In contrast, the PW and P correlation functionals have a strong theoretical background, both respecting all the above-mentioned conditions, except the vanishing-correlation one.

In light of our results, it is evident that conditions a and b are dominant for the description of the electronic properties of systems including heavy metals. So we will not further consider the LYP correlation functional. Furthermore, to minimize the spurious effects arising from the self-interaction (condition c), we will use only the P correlation functional, which provides an error lower than the PW functional.[71]

Molecular Structure Calculations. There has been an extensive debate in the literature regarding the exact conformation of the LnX_3 species,[42,45] and some authors have tried to relate the most stable structure to the nature (ionic or covalent) of the bonding.[45,74,75] Unfortunately, the interpretation of the experimental data from infrared spectroscopy or electron diffraction are sometimes contradictory,[45] owing to the flexible nature of these molecules. For instance, electron diffraction experiments only give averaged values about the bend angle, and the low-frequency bending mode may not be detected.[42] So we prefer to compare our results with published computations rather than with experimental data, allowing readers to draw their own conclusions. The geometrical parameters of the most stable conformation of each species, i.e., the Ln−X bond length and the X−Ln−X valence angle, have been reported in Table 3, together with experimental[40,42] and post-HF data.[41,44,46−48] The BP/QR and the B3P/RECP (see Table 3) computations differ by both the treatment of the exchange term and the type of relativistic correction. We have therefore carried out additional BP/RECP geometry optimizations in the same framework as the B3P/RECP calculations. Without entering in a tedious analysis of these results, we only note that DFT interatomic distances are usually better than those provided by post-HF computations. In particular, the mean absolute error on the bond length is 0.021 Å for the BP/QR approach, 0.025 Å for the B3P/RECP, and 0.035 for BP/RECP, whereas it is 0.033 for CISD+Q computations. Previously published SCH computations,[48] carried out with the popular B3LYP model and the same RECP's, provide an error of 0.036 Å, pointing out, once again, the key role played by the correlation functionals in the performances of DFT approaches, when applied to heavy-metal chemistry. The nature of relativistic corrections is also determinant to accurately reproduce experimental geometries: the frozen core methodology (BP/QR) clearly gives better results that all other RECP-based computations, either in the DFT or HF framework.

As expected, the energy differences between C_{3v} and D_{3h} structures, corrected for zero-point energy (ZPE) effects, are very low, being always below 1 kcal/mol. In particular the largest difference is found for LaF_3, where the C_{3v} structure is more stable by 0.05 kcal/mol (at the B3P level). Nevertheless, a general trend can be observed from these computations, whatever the DFT method. All LaX_3 molecules are pyramidal, as well as GdF_3 and LuF_3, whereas $GdBr_3$, GdI_3, and LuX_3, X = Cl, Br, I, are planar. This means that the planar geometry is favored for the heavier lanthanides, and this trend may be correlated to the contribution of the Ln^{3+} d and s valence orbitals to the bonding (see below).

Some calculations including the SO coupling have been carried out varying the geometrical parameters for some molecules ($LaCl_3$, LaI_3, and LuI_3), and no influence has been detected on the position of the equilibrium geometry.

The harmonic vibrational frequencies were also computed for the whole series of molecules, in both pyramidal and planar conformations. The calculated harmonic wavenumbers for the most stable structure of the whole series of molecule are collected in Table 4, together with experimental data, either measured or estimated.[40,42,43] For all the molecules belonging to C_{3v} symmetry, the corresponding D_{3h} saddle point was also characterized, whose imaginary frequency corresponding to the ν_2 bending mode (out-of-plane mode) is generally around 100i cm^{-1}). The agreement with experimental data is satisfactory for all the considered DFT approaches, the mean absolute error

TABLE 4: Calculated Harmonic Frequencies (cm^{-1}) with BP and B3P, Experimental Values (Estimated Values in Italics[40]), and Other Theoretical Calculations: CAS[41,47] and MP2[43]

	method	ν1	ν2	ν3	ν4
LaF_3	exptl[a]	528	81	497	130
	BP	521	63	496	113
	B3P	517	83	485	127
	CAS	545	53	542	129
$LaCl_3$	exptl	335/337	51/59	300/333	72/74
	BP	320	30	309	65
	B3P	331	45	323	80
	CAS	323	26	301	72
	MP2	332	35	321	70
$LaBr_3$	exptl	220/232	30/35	190	47
	BP	233	26	196	42
	B3P	236	46	208	66
	MP2	248	22	205	45
LaI_3	exptl	*186*	*28*	*177*	*44*
	BP	183	21	132	28
	B3P	177	26	136	30
	MP2	150	19	201	33
GdF_3	exptl[a]	573	97	552	136
	BP	563	48	549	138
	B3P	569	117	553	138
	CAS	577	116	568	134
$GdCl_3$	exptl	338	56	326	84
	BP	337	32	322	73
	B3P	333	43	331	77
	CAS	336	45	314	77
$GdBr_3$	exptl[a]	*268*	*44*	*257*	*66*
	BP	240	17	194	45
	B3P	238	47	238	64
GdI_3	exptl[a]	*188*	*31*	*181*	*46*
	BP	184	19	126	28
	B3P	193	30	140	37
LuF_3	exptl[a]	*598*	*106*	*585*	*147*
	BP	580	43	571	142
	B3P	589	60	573	150
	CAS	596	55	594	135
	MP2	629	42	622	141
$LuCl_3$	exptl[a]	*342*	*60*	*331*	*88*
	BP	351	25	331	82
	B3P	340	73	323	77
	CAS	349	52	323	87
	MP2	368	41	342	78
$LuBr_3$	exptl[a]	*271*	*48*	*263*	*70*
	BP	248	20	201	51
	B3P	252	36	198	53
LuI_3	exptl[a]	*191*	*34*	*185*	*49*
	BP	184	28	130	34
	B3P	195	29	145	37

[a] See ref 80.

being 18 cm^{-1} for the BP model and 13 cm^{-1} for the B3P approach. Similar errors, even if obtained over a smaller set of molecules, are found at the MP2 (18 cm^{-1}) and at the CAS (13 cm^{-1}) level.[41,43,47] The largest deviations from experimental data are found for some low frequencies, which have not been measured directly but only estimated by an extrapolation procedure.[40,42] For instance, an error of 46 cm^{-1} is found for the ν_2 mode of LuF_3 at the B3P level, and BP computation places the ν_3 mode of $LuBr_3$ 62 cm^{-1} below the experimental estimate. Similar differences are found at any level of computation, including post-HF methods, suggesting either a revision of the evaluation of extrapolated frequencies or the influence of the anharmonicity.

TABLE 5: Atomization Energies (eV) from DFT Computations, Experimental Data,[74] and CISD+Q Calculations[44]

	BP	ΔSO[b]	B3P	best estimate[a]	CISD+Q	exptl
LaF_3	22.02	+1.23	19.20	20.43	18.17	19.81
$LaCl_3$	16.19	+0.59	15.18	15.77	13.80	15.88
$LaBr_3$	14.50	+0.11	13.70	13.81	11.86	13.71
LaI_3	12.32	−0.35	12.02	11.67	9.55	11.28
GdF_3	21.15		20.03		18.16	18.81
$GdCl_3$	15.43		15.97		13.24	15.14
$GdBr_3$	13.73		13.43		12.28	13.06
GdI_3	11.52		11.20		8.96	10.33
LuF_3	21.00	+1.17	19.56	20.73	18.21	18.44
$LuCl_3$	15.29	+0.54	16.02	16.56	13.15	15.10
$LuBr_3$	14.30	−0.67	14.60	13.93	11.15	12.80
LuI_3	11.80	−0.90	11.65	10.75	8.78	10.67

[a] B3P + SO correction from BP computations. [b] SO contribution, evaluated at the BP level.

Apart from the good agreement of structural parameters compared to experimental data, we have also checked the ability of our approach to reproduce thermodynamic quantities, by computing the atomization energies of the LnX_3 molecules, whose values are experimentally known.[10] These energies were calculated for the most stable conformation of each species and corrected for ZPE effects. The atomic ground states were computed within spherical symmetry and including spin polarization.[76]

The results are reported in Table 5. As can be seen, all the DFT computations provide results that are in better agreement with experimental data than the post-HF values. The absolute mean error is 1.2 eV at the BP level and 0.85 eV at the B3P level, while CISD+Q computations provide a deviation of 1.5 eV.[34] The inclusion of SO effects at the BP level further reduces the discrepancy with experiments, and the best estimate (mean absolute error, 0.7 eV) was obtained with the B3P results corrected by the SO contribution, the latter being estimated from the BP/SO and BP/Sc computations. In particular, it must be noted that the calculations including SO effects are significantly more reliable for the molecules containing heavy halogens (from Cl to I, mean relative error 0.5 eV) whereas the poor agreement obtained for the fluoride derivatives may be related first to the worse agreement already observed for the scalar computations and also to the inadequacy of the *jj* coupling to describe light elements.

For the three elements computed here, the *jj* coupling is not yet adequate, except maybe for the heaviest lanthanide, and the best treatment of SO effects would be an intermediate coupling. For trivalent lanthanides with partial filling of the 4f shell, such as Nd^{3+} ($4f^3$) or Eu^{3+}($4f^6$), the LS states arising from this electron configuration are given by combinations of various 4f subconfigurations.[70] This is why the method given by Desclaux, i.e., evaluating an average energy, deserves to be tested on such systems. Anyway, these orbitals being almost core like, the influence of varying 4f occupations on structural properties or on the nature of the bonding, the properties that we are interested in, is not expected to be determining. This will be further tested for Nd^{3+} and Eu^{3+} in either the scalar or SO scheme.

Electronic Structure of LnX_3. Starting from the BP results, a general scheme of the interactions between the Ln and the X atoms may be drawn, in which three main contributions may be evidenced: the interaction between the inner 5p electrons of the lanthanide and the valence *n*s orbitals of the halogens, the contribution arising from the 4f atomic orbitals (AOs), and finally the interaction between the valence occupied *n*p orbitals (X) and the 5d and 6s electrons of the lanthanide.

TABLE 6: Orbital Energies (Absolute Values, eV) and Ln Orbital Character (%) of the Three *n*p-Based MO's of LnX_3, Ln = La, Gd, Lu and X = Cl and I

		Cl		I	
	MO	*E*	Ln orbital character	*E*	Ln orbital character
LaX_3	a1/a′1	−8.619	4.7 d_{z^2}, 2.7 6s	−7.939	5.7 d_{z^2}, 9.2 6s
	e1/e′1	−8.410	14.3 (d_{xy}, $d_{x^2-y^2}$)	−7.543	19.9 (d_{xy}, $d_{x^2-y^2}$)
	e1/e″1	−8.027	8.6 (d_{xz}, d_{yz})	−7.119	11.6 (d_{xz}, d_{yz})
GdX_3	a1/a′1	−8.866	3.7 d_{z^2}, 5.8 6s	−8.335	4.2 d_{z^2}, 16.6 6s
	e1/e′1	−8.664	15.1 (d_{xy}, $d_{x^2-y^2}$)	−7.752	15.9 (d_{xy}, $d_{x^2-y^2}$)
	e1/e″1	−8.198	9.9 (d_{xz}, d_{yz})	−7.205	10.3 (d_{xz}, d_{yz})
LuX_3	a1/a′1	−9.447	2.2 d_{z^2}, 9.4 6s	−8.792	2.2 d_{z^2}, 24.8 6s
	e1/e′1	−8.853	12.9 (d_{xy}, $d_{x^2-y^2}$)	−7.841	13.6 (d_{xy}, $d_{x^2-y^2}$)
	e1/e″1	−8.313	9.5 (d_{xz}, d_{yz})	−7.230	12.2 (d_{xz}, d_{yz})

[a] All values are computed at the BP level. In the case of the open-shell derivatives of Gd, the α orbitals are reported.

Let us analyze in some detail these interactions. First, a four-electron/two-orbital repulsion is observed between the symmetry-adapted combinations of 5p (Ln) and *n*s (X) orbitals, modulated by the energy gap between these AO's. The energies of these 5p (Ln) and *n*s (X) orbitals were evaluated in the LnX_3 molecular calculations, from the noninteracting combinations of these AO's. In particular this repulsive interaction is very strong in GdF_3, in which the 5p orbitals of the metal (−28.5 eV) are very close to the 2s orbital of F (−27.9 eV). Weaker, but still significant repulsions are found between La and Cl or Br. Finally, for Lu derivatives, the large energy gap between the 5p and *n*s levels precludes any orbital interaction, except for LuF_3. From a technical point of view, this shows that an accurate description of the Ln−X interactions can be obtained only through an explicit description of 5p electrons, i.e., reducing the frozen core of the metal.

Not surprisingly, the energies of the 4f AO's decrease from La (−2.0 eV) to Gd (−10.2 eV) and to Lu (−10.8 eV) corroborating the well-known chemical inertness of these electrons, owing to the small radial extension of these orbitals. In fact, there is almost no mixing with the *n*p orbitals in the case of La species or in the case of Gd and Lu derivatives with Br and I. In contrast, strong mixings were observed in the case of GdX_3 and LuX_3 with X = F and Cl, owing to the very close proximity of the 4f energy levels of Gd or Lu with those of F(2p) and Cl(3p). Anyway the corresponding overlaps are weak (0.01−0.04), whereas the overlaps between *n*p and 5d orbitals are 10 times larger. This mixing of 4f AO's with ligand orbitals, owing to an accidental degeneracy, has already been observed in photoelectron spectroscopy of LnX_3 species as well as in the associated Xα−discrete variational computations.[3]

The most important orbital interactions for describing the Ln−X bonding arise in the X valence region, where the resulting MO's are mainly of p-character, with various contributions of Ln valence electrons involving essentially the 5d and 6s AO's. In trigonal symmetry, three MO's describe the main bonding features: the a_1 orbital formed by the interaction between the 6s, d_{z^2} and the fully symmetric combination of *n*p orbitals belonging to the X atoms, and the e_1 (or e'_1 and e''_1 in D_{3h} conformation) MO's π-bonding orbitals, formed by the two sets of $5d_{xz}$, $5d_{yz}$, and $5d_{xy}$, $5d_{x^2-y^2}$ AO's of the lanthanide.

The orbital energies and the contributions (%) of the Ln AO's in these *n*p-based MO's are reported in Table 6 for some representative LnX_3 compounds. Several trends may be pointed out, either along the halogen series, for a given lanthanide, or along the Ln series, for a fixed halogen. As an example, we have plotted in Figure 1 the evolutions of the 6s and $5d_{z^2}$ characters within the a_1 orbital for the three lanthanide elements as a function of the halogen. The symmetry was taken as C_{3v} for all species, even for molecules characterized by a D_{3h} equilibrium structure, the results being similar in both conformations.

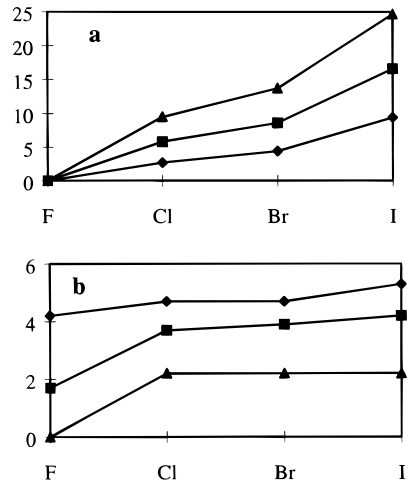

Figure 1. Contributions from Ln atomic orbitals (6s, 1a; $5d_{z^2}$,1b) to the σ-bonding orbitals in LaX_3 (◆), GdX_3 (■), and LuX_3 (▲) as resulting from BP computations.

As can be seen from Table 6 and Figure 1, both the 6s and 5d characters in the Ln−X bond increase when going to the heaviest halogens, for a given Ln, owing to the more diffuse *n*p valence orbitals. This effect is much more pronounced for the 6s than for the $5d_{z^2}$ orbital. For the other 5d orbitals, the trend parallels that of $5d_{z^2}$, with slightly larger contributions (ca. 10−20%, see Table 6).

Other interesting trends may be observed concerning the evolutions through the lanthanide series. The 6s character increases from La to Lu for a given halogen (except F), and in the case of the iodide species, it is reinforced from 9.2% for La, up to about 25% for Lu. Conversely, the 5d character shows either an almost constant behavior or a decrease depending on the halogen. This relative behavior of the 6s and $5d_{z^2}$ orbitals had been already described in the literature, either in experimental[3] or theoretical[75] results. This is related to the variation of the 6s and 5d orbitals through the lanthanide series. The energy level of the 6s AO decreases from La to Lu thus bringing the 6s AO closer in energy to the *n*p orbitals of the halogen. In contrast, the 5d orbitals are more diffuse: the indirect effect of contraction of the 6s increases the shielding of the nuclear charge thus destabilizing the 5d orbitals. The electron transfer from X^- to Ln^{3+} follows the same trends, thus giving rise to the above-mentioned variations observed in the bonding depending on Ln and X.

This balance between the relative 6s and $5d_{z^2}$ characters may be responsible for the change in the symmetry of the most stable

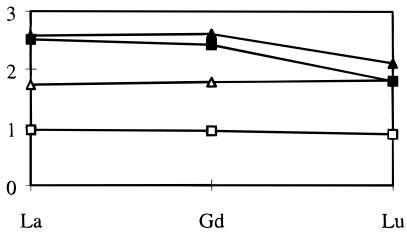

Figure 2. Mulliken and NPA atomic charges on Ln for the LnF_3 (△, Mulliken; ▲, NPA) and LnI_3 (□, Mulliken; ■, NPA) (Ln = La, Gd, Lu) complexes computed at the B3P level.

conformation, and this phenomenon has been mentioned in previous calculations.[75,48] When the contribution of the $5d_{z^2}$ is higher than that of the 6s orbitals, the overlaps with *n*p orbitals are larger in the bent conformation. When the 6s character becomes predominant, i.e., for the heavier Ln and X, the overlap with the symmetry-adapted combination of *n*p orbitals increases when going from a bent to a planar conformation. These changes in the overlaps were checked in the BP computations: in the case of $LaCl_3$, the $5d_{z^2}$/3p overlap is 0.258 for C_{3v} and 0.157 for D_{3h}, whereas for LuI_3, the 6s/5p overlap is 0.477 for C_{3v} and 0.492 for D_{3h}. Such subtle effects determine the small energy difference between the two conformations. Finally, it should be noted that the content of the MO's with $5d_{xz}-5d_{yz}$ and $5d_{xy}-5d_{x^2-y^2}$ characters, i.e., the e'_1 (and e''_1 orbitals) do not vary as much: their contributions for all the species vary only by a few percent, depending on the lanthanide and halogen atoms.

All these results suggest that the Ln−X bond has a strong ionic character, which decreases in going from La to Lu, whereas the covalent character is enhanced by the presence of soft ligands, such as I. These results are at variance with previous published data obtained by standard ab initio computations, which strongly support the idea of a covalent Ln−X bond.[74] This statment is based on standard population analyses, such as the popular Mulliken one (MPA).[77] Without going into details, the theoretical limitations of such an analysis are well-known (see, for instance, ref 78). In contrast, the NPA provides electronic populations that are more reliable and stable to computational parameters (e.g., basis sets).[79] This situation is well-evidenced in Figure 2, where are plotted the Mulliken and the NPA charges for the Ln atoms, obtained at the B3P level, for the fluorine and the iodine complexes in their minimum energy conformation. From this plot, it is quite clear that MPA and NPA give drastically different descriptions of the Ln−X bond. In fact, the Mulliken charges suggest the presence of a bond with a significative covalent character for the fluorine complex ($q = 1.8|e^-|$) and a totally covalent bond for the iodine complex ($q < 1.0|e^-|$). Furthermore, the charge on the metal is almost constant along the whole lanthanide series. In contrast, NPA indicates a strong ionic bond ($q > 2.5|e^-|$), which significantly decreases in going from Gd to Lu ($q = 2.0|e^-|$ for LuI_3).

Similar conclusion can be drawn starting from the NRT analysis, carried out on B3P results. Figure 3 shows the ionic contribution to the Ln−X bond for all the considered lanthanide complexes. From this plot, it is quite apparent that the ionic contribution is almost the same for all complexes of Gd and Lu, while it is somewhat larger for the La derivatives. This discrepancy increases in going from F to Cl, thus confirming the strong relationship between the strength of electrostatic forces and the molecular arrangement.

These results are quite puzzling, since chemical intuition would suggest that the hardness of Ln^{3+} increases with the number of electrons, thus favoring a ionic bonding interaction. A better quantitative evaluation of the nature of the bonding can be obtained by a more detailed energetic analysis using the transition-state method.[56]

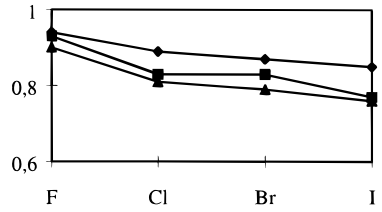

Figure 3. Variation of the ionic character (1, ionic bond; 0, covalent bond) of the Ln−X bond in the trihalide complexes of La (◆), Gd (■), and Lu (▲) as resulting from B3P computations.

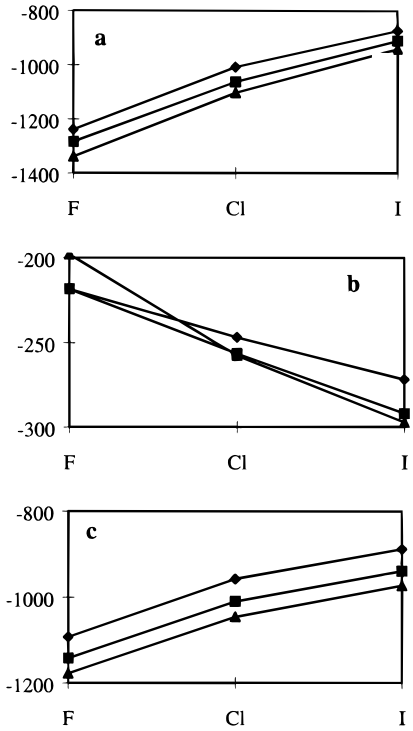

Figure 4. Electrostatic interactions (a), orbital interactions (b), and total bonding energies (c), in kcal/mol, vs the halogen atom (F, Cl, I), for LaX_3 (◆), GdX_3 (■) and LuX_3 (▲) as resulting from BP computations.

The evolution of the electrostatic and of the orbital interaction terms, together with the total bonding energy for La, Gd, and Lu derivatives, has been plotted as a function of the halogen for F, Cl, and I in Figure 4. As expected, the stabilization due to electrostatic interactions decreases when going to the softer iodide ligand, whatever the lanthanide. The second interesting trend, which was expected from the increase of hardness when going to the end of the Ln series, is the greater stabilization of the Lu species owing to ionic interactions compared to Gd and La. The orbital interactions are more stabilizing when going from F to I, and this is due in particular to the increase of the participation of the 6s orbital in the valence orbitals.

As can be seen, these two energetic terms exhibit opposite trends, but clearly the predominant term is the electrostatic contribution, with a destabilization of about 400 kcal/mol from F to I. In turn, the orbital interactions brings about a stabilizing effect of less than 100 kcal/mol. Thus we can conclude that the predominant effect in the stabilization of these species is the electrostatic interaction: this is reflected in the evolution of the total bonding energy, which parallels that of the electrostatic term.

4. Conclusion

We have presented here the first DFT computations on the LnX_3 species, which have already been extensively studied by other ab initio or extended Hückel methods. We have shown here the ability of density functional calculations to satisfactorily reproduce both structural and thermodynamic experimental data on these compounds containing heavy atoms. Comparable results are obtained by both approaches employed to take into acount relativistic effects, namely, the RECP-based methodology and the frozen core/quasi-relativistic computation. It is interesting to note that the RECP used here was obtained by fitting fully relativistic HF data and has been used as such in the DFT computations without any modification.

Another point deserving interest is that the standard gradient-corrected functionals as well as SCH methods are successful to describe the electronic properties of species containing heavy metal atoms, characterized by large correlation and relativistic effects.

Finally, it must be pointed out that one of the major advantages in using DFT relies on their ability to provide a "chemical" analysis of the bonding, in terms of a quantitative determination of the electrostatic and covalent interactions. In this connection, we have thus shown that the bonding in the LnX_3 species is mainly ionic, whatever the lanthanide and the halogen, and that the increase of covalency induced by more polarizable ligands is too weak to provide any stabilization due to orbital interactions.

The study of 5f analogues is under way, within the same framework, with in particular a careful examination of the influence of 5f occupations on the bonding, as these orbitals are expected to be more diffuse and to be more involved in the bonding. On the basis of these computations, more complex lanthanide and actinide species will then be studied.

Acknowledgment. The authors thank Pr. Robert Subra (University J. Fourier, Grenoble, France) and Pr. Vincenzo Barone (Università "Federico II", Naples, Italy) for fruitful discussions and helpful comments.

References and Notes

(1) Di Bella, S. G., A.; Lanza, G.; Fragala, I.; Stern, D.; Marks, T. J. *Organometallics* **1994**, *13*, 3810−3815.
(2) Lee, E. P. F.; Potts, A. W.; Bloor, J. E. *Proc. R. Soc. London* **1982**, *A381*, 373−393.
(3) Ruscic, B.; Goodman, G. L.; Berkowitz, J. *J. Chem. Phys.* **1983**, *78*, 5443.
(4) Seth, M.; Dolg, M.; Fulde, P.; Schwerdtfeger, P. *J. Am. Chem. Soc.* **1995**, *117*, 6597−6598.
(5) Pykko, P. *Inorg. Chim. Acta* **1987**, *139*, 243−245.
(6) Pepper, M.; Bursten, B. E. *Chem. Rev.* **1991**, *91*, 719−741.
(7) Nash, C. S.; Bursten, B. E. *New J. Chem.* **1995**, *19*, 669−675.
(8) Burns, C. J.; Bursten, B. E. *Comments Inorg. Chem.* **1989**, *9*, 61−93.
(9) Kaltsoyannis, N.; Bursten, B. E. *Inorg. Chem.* **1995**, *34*, 2735−2744.
(10) Nash, K. L. *Separation chemistry for lanthanides and trivalent actinides*; Elsevier Science B. V: Amsterdam, 1994; Vol. 18.
(11) Pyykko, P. *Chem. Rev.* **1988**, *88*, 563−594.
(12) Hess, B. A. *Ber. Bunsen-Ges. Phys. Chem.* **1997**, *101*, 1−10. Dolg, M.; Stoll, H. *Handbook of Chemistry and Physics of Rare-Earth*; Gschneidner, K. A., Jr., Eyring, L., Eds.; Elsevier: Amsterdam, 1996; Vol. 22, Chapter 152.
(13) Dyall, K. G.; Taylor, P. R.; Faegri, K. J.; Harry, P. *J. Chem. Phys.* **1991**, *95*, 2583−2594.
(14) Malli, G. L.; Styszynski, J. *J. Chem. Phys.* **1994**, *101*, 10736−10745.
(15) Visscher, L.; Dyall, K. G. *J. Chem. Phys.* **1996**, *104*, 9040.
(16) Foldy, L. L.; Wouthuysen, S. A. *Phys. Rev.* **1950**, *78*, 29.
(17) Douglas, M.; Kroll, N. M. *Ann. Phys.* **1974**, *82*, 89.
(18) Ermler, W. C.; Lee, Y. S.; Christiansen, P. A.; Pitzer, K. S. *Chem. Phys. Lett.* **1981**, *81*, 70.
(19) Dolg, M.; Stoll, H.; Savin, A.; Preuss, H. *Theor. Chim. Acta* **1989**, *75*, 173−194.
(20) Hay, J. P.; Wadt, W. R. *J. Chem. Phys.* **1985**, *82*, 299−310.
(21) Cundari, T. R.; Stevens, W. J. *J. Chem. Phys.* **1993**, *98*, 5555.
(22) Ziegler, T. *Can. J. Chem.* **1995**, *73*, 743.
(23) Jonas, V.; Thiel, W. J. *J. Chem. Phys.* **1995**, *102*, 8474.
(24) Eriksson, L. A.; Pettersson, L. G. M.; Siegbahn, P. E. M.; Wahlgren, U. J. *J. Chem. Phys.* **1995**, *110*, 872.
(25) Castro, M.; Salahub, D. R.; Fournier, R. *J. Chem. Phys.* **1994**, *100*, 8233.
(26) Delly, B.; Wrinn, M.; Luthi, H. P. *J. Chem. Phys.* **1994**, *100*, 5785.
(27) Adamo, C.; Lelj, F. *J. Chem. Phys.* **1994**, *103*, 10605.
(28) Barone, V.; Adamo, C. *J. Phys. Chem.* **1996**, *100*, 2094.
(29) Holthausen, M. C.; Heinemann, C.; Cornehl, H. H.; Koch, W.; Schwarz, H. J. *J. Chem. Phys.* **1995**, *102*, 4931.
(30) Becke, A. D. *J. Chem. Phys.* **1993**, *98*, 5648.
(31) Ziegler, T.; Tschinke, V.; Baerends, E. J.; Snijders, J. G.; Ravenek, W. *J. Phys. Chem.* **1989**, *93*, 3050−3056.
(32) van Leeuwen, R.; van Lenthe, E.; Baerends, E. J.; Snijders, J. G. *J. Chem. Phys.* **1994**, *101*, 1271.
(33) Russo, T. V.; Martin, R. L.; Hay, P. J. *J. Phys. Chem.* **1995**, *99*, 17085.
(34) Wang, S. G.; Pan, D. K.; Schwarz, W. H. E. *J. Chem. Phys.* **1995**, *102*, 9296−9308.
(35) ADF 2.3.0. Theoretical Chemistry, Vrije Universiteit, Amsterdam.
(36) Baerends, E. J. *Chem. Phys.* **1973**, *2*, 41.
(37) te Velde, G.; Baerends, E. J. *J. Comput. Phys.* **1992**, *99*, 84.
(38) Fonseca Guerra, C.; et al. *METECC-95* **1995**, 305.
(39) Spiridinov, V. P.; Gershikov, A. G.; Lyutsarev, V. S. *J. Mol. Struct.* **1990**, *221*, 79.
(40) Myers, C. E.; Graves, D. T. *J. Chem. Eng. Data* **1977**, *22*, 436.
(41) Di Bella, S.; Lanza, G.; Fragala, I. L. *Chem. Phys. Lett.* **1993**, *214*, 598.
(42) Hargittai, M. *Coord. Chem. Rev.* **1988**, *91*, 35−88.
(43) Kovacs, A.; Konings, R. J. M.; Booij, A. S. *Chem. Phys. Lett.* **1997**, *268*, 207−212.
(44) Dolg, M.; Stoll, H.; Preuss, H. *J. Mol. Struct.*: *THEOCHEM* **1991**, *235*, 67.
(45) Molnar, J.; Hargittai, M. *J. Phys. Chem.* **1995**, *99*, 10780−10784.
(46) Cundari, T. R.; Sommerer, S. O.; Strohecker, L. A.; Tipett, L. *J. Chem. Phys.* **1995**, *103*, 7058.
(47) Lanza, G.; Fragala, I. L. *Chem. Phys. Lett.* **1996**, *255*, 341.
(48) Adamo, C.; Maldivi, P. *Chem. Phys. Lett.* **1997**, *268*, 61−68.
(49) Baerends, E. J.; et al. *Chem. Phys.* **1973**, *2*, 41.
(50) Dirac, P. A. M. *Proc. Cambridge Philos. Soc.* **1930**, *29*, 376.
(51) Vosko, S. H.; Wilk, L.; Nusair, M. *Can. J. Phys.* **1980**, *58*, 1200.
(52) Lee, C.; Yang, W.; Parr, R. G. *Phys. Rev. B* **1988**, *37*, 785.
(53) Perdew, J. P. *Phys. Rev. B* **1986**, *33*, 8822.
(54) Perdew, J. P. *Phys. Rev. B* **1992**, *46*, 6671.
(55) Becke, A. D. *Phys. Rev. A* **1988**, *38*, 3098.
(56) Ziegler, T.; Rauk, A. *Theor. Chim. Acta* **1977**, *46*, 1.
(57) Snijders, J. G.; Vernooijs, P.; Baerends, E. J. *At. Data Nucl. Data Tables* **1982**, *26*, 483.
(58) Krijn, J.; Baerends, E. J. Internal Report, V. U., Amsterdam, 1984.
(59) Stevens, W. J.; Krauss, M.; Basch, H.; Jasien, P. G. *Can. J. Chem.* **1992**, *70*, 288.
(60) Stevens, W. J.; Basch, H.; Krauss, M. *J. Chem. Phys.* **1984**, *81*, 6026.
(61) Frisch, M. J.; Trucks, G. W.; Schlegel, H. B.; Gill, P. M. W.; Jonhson, B. G.; Robb, M. A.; Cheeseman, J. R.; Keith, T. A.; Petersson, G. A.; Montgomery, J. A.; Raghavachari, K.; Al-Laham, M. A.; Zakrewski, V. G.; Ortiz, J. V.; Foresman, J. B.; Cioslowski, B.; Stefanov, B.; Nanayakkara, A.; Challacombe, M.; Peng, C. Y.; Ayala, P. Y.; Chen, W.; Wong, M. W.; Andres, J. L.; Replogle, E. S.; Gomperts, R.; Martin, R. L.; Fox, D. J.; Binkley, J. S.; Defrees, D. J.; Baker, J.; Stewart, J. P.; Head-Gordon, M.; Gonzalez, C.; Pople, J. A. *Gaussian 94*; Pittsburgh, PA, 1995.
(62) Glendening, E. D.; Badenhoop, J. K.; Reed, A. E.; Carpenter, J. E.; Weinhold, F. NBO 4.0 Theoretical Chemical Institute, University of Wisconsin; Madison, WI, 1996.
(63) Glendening, E. D.; Weinhold, F. Technical Report WIS-TCI-803, Theoretical Chemistry Institute, University of Wisconsin, Madison, WI, 1994.
(64) Duffy, P.; Chong, D. P.; Casida, M. E.; Salahub, D. R. *Phys. Rev. B.* **1994**, *50*, 4707.
(65) Goerling, A. *Phys. Rev. A.* **1996**, *54*, 3912.
(66) Kotochigova, S.; Levine, Z. H.; Shirley, E. L.; Stiles, M. D.; Clark, C. W. *Phys. Rev. A* **1997**, *55*, 191−199.
(67) Kaltsoyannis, N. *J. Chem. Soc., Dalton Trans.* **1997**, 1−11.
(68) Desclaux, J.-P.; Moser, C. M.; Verhaegen, G. *J. Phys. B: At. Mol. Opt. Phys.* **1971**, *4*, 296−310.

(69) Desclaux, J.-P. *At. Data Nucl. Data Tab.* **1973**, *12*, 311−406.
(70) *Atomic Energy Levels. The rare earth elements*; Martin, W. C., Zalubas, R., Hagan, L., Eds.; U.S. Government Printing Office: Washington, DC, 1978; Vol. 60. Available on Internet: http://physics.nist.gov.
(71) Becke, A. D. *J. Chem. Phys.* **1996**, *104*, 1040.
(72) Laming, G. J.; Termath, V.; Handy, N. J. *J. Chem. Phys.* **1993**, *99*, 8765.
(73) Adamo, C.; Barone, V. *Chem. Phys. Lett.* **1997**, *276*, 242.
(74) Myers, C. E. *Inorg. Chem.* **1975**, *14*, 199.
(75) Myers, C. E.; Norman II, L. J.; Loew, L. M. *Inorg. Chem.* **1978**, *17*, 1581.
(76) Baerends, E. J.; Branchadell, V.; Sodupe, M. *Chem. Phys. Lett.* **1997**, *265*, 481.
(77) Mulliken, R. S. *J. Chem. Phys.* **1955**, *23*, 1833.
(78) Dronskowski, R.; Bloechl, P. E. *J. Phys. Chem.* **1993**, *97*, 8617.
(79) Reed, A. E.; Curtiss, L. A.; Weinhold, F. *Chem. Rev.* **1988**, *88*, 899.
(80) Hauge, R. H.; Hastie, J. W.; Margrave, J. L. *J. Less-Common Met.* **1971**, *23*, 359.